Pergamon

Tetrahedron 56 (2000) 3353–3364

TETRAHEDRON

Syntheses and Spectroscopic Studies of Novel Chlorins with Fused Quinoxaline or Benzimidazole Ring Systems and the Related Dimers with Extended Conjugation[1]

Andrei N. Kozyrev,[a] V. Suresh,[b] Suresh Das,[b] Mathias O. Senge,[c] Masayuki Shibata,[d] Thomas J. Dougherty[a] and Ravindra K. Pandey[a,e,*]

[a]*Chemistry Division, Photodynamic Therapy Center, Roswell Park Cancer Institute, Buffalo, NY 14263, USA*
[b]*Photochemistry Research Unit, Regional Research Laboratory, Trivandrum 695 019, India*
[c]*Institute Fur Chemie, Organische Chemie (WEO2), Freie Universitate, Berlin, Takustr. 3, D-14195, Germany*
[d]*Molecular and Cellular Biophysics, Roswell Park Cancer Institute, Buffalo, NY 14263, USA*
[e]*Department of Nuclear Medicine, Roswell Park Cancer Institute, Buffalo, NY 14263, USA*

Received 15 February 2000; accepted 23 March 2000

Abstract—Condensation of 13^2-oxopyropheophorbide *a* **1** with various aromatic diamines under acid-catalyzed conditions afforded a series of novel chlorins with fused quinoxaline or benzimidazole polyaromatic ring systems. This methodology was extended for the preparation of laterally bridged pyropheophorbide *a* dimers. Reaction of **1** with 1,2,4,5-benzenetetramine produced a bis-quinoxaline-bridged symmetrical chlorin dimer **16** and an unsymmetrical benzimidazole/pyrazine bridged analog **17**. Spectroscopic data of novel conjugated dimers show a significant perturbation of the extended bis-chlorin π-system in a coplanar arrangement. The excited state properties of some novel chlorin derivatives **4**–**6**, **14**, and dimers **16** and **17**, which contain two laterally bridged pheophorbides have been examined. Compounds **4**–**6**, **16** and **17** are weakly fluorescent (ϕ_f=0.08–0.16) with singlet state lifetimes ranging from 2–5 ns. These compounds show high intersystem crossing efficiencies (ϕ_T=0.39–0.58). A close match was observed between the quantum yields for singlet oxygen generated and their triplet quantum yields. The excited state of **14** undergoes deactivation mainly through a non-radiative route with fluorescence and triplet state quantum yields being negligible.The monomeric and dimeric structures of annulated chlorins show a characteristic vinylogous-type enolization of the 12-methyl group adjacent to the fused ring systems. The crystallographic and the modeling studies of these novel chlorins indicated a rigid construction of condensed aromatic heterocycles in a planar arrangement.

Introduction

Chlorins possessing fused aromatic rings have received increased attention in recent years.[2–6] The interest in these tetrapyrroles is based on their potential use as second generation photosensitizers for photodynamic therapy (PDT) of malignant tumors. Chlorins containing conjugated exocyclic ring systems, e.g. benzochlorins,[3,7] purpurins[7] and *N*-alkylimide analogs of purpurin-18[8] and pheophorbides[9] have been reported as effective photosensitizers with significant anticancer activity. The introduction of aromatic ring systems fused into a chlorin molecules generally results in red shift of their respective long-wavelength absorption due to extended conjugation.[10] This optical characteristic is especially important for achieving a photosensitizer with deeper tissue penetration. It has been shown that incorporation of rigidly connected aromatic system can cause a distortion of chlorin macrocycle plane, that can be one of the reasons of their unique photophysical characteristics.[11] Versatility of the attachment of various aromatic fused rings at different positions of the chlorin macrocycle can bring a significant variation in properties of this highly interesting class of compounds.

Recently, we reported a facile method for the synthesis of methyl 13^2-oxopyropheophorbide *a* **1** via LiOH-promoted allomerization of pyropheophorbide *a*.[12] It was observed that extremely electron deficient diketone **1** readily react with diazomethane to produce a novel chlorin with a conjugated oxocyclohexene ring system named as verdinochlorins. This class of compounds exhibited an unexpectedly large red shift of their absorption Q_y-band.[13] To explore the reactivity of a α-quinone functionality, we planned to use **1** as a starting material for the preparation of pyropheophorbide *a* derivatives with fused aromatic rings via the quinoxaline condensation with aromatic diamines as the building blocks. In this paper we describe a successful application of this methodology for the preparation of novel

Keywords: photosensitizers; chlorin containing polyaromatic rings; laterally bridged pheophorbide *a* dimer; vinylogous enolization; photophysical properties; X-ray studies; molecular modeling.
* Corresponding author. Tel.: +1-716-845-3203; fax: +1-716-845-8920; e-mail: rpandey@sc3103.med.buffalo.edu

0040–4020/00/$ - see front matter
PII: S0040-4020(00)00256-8

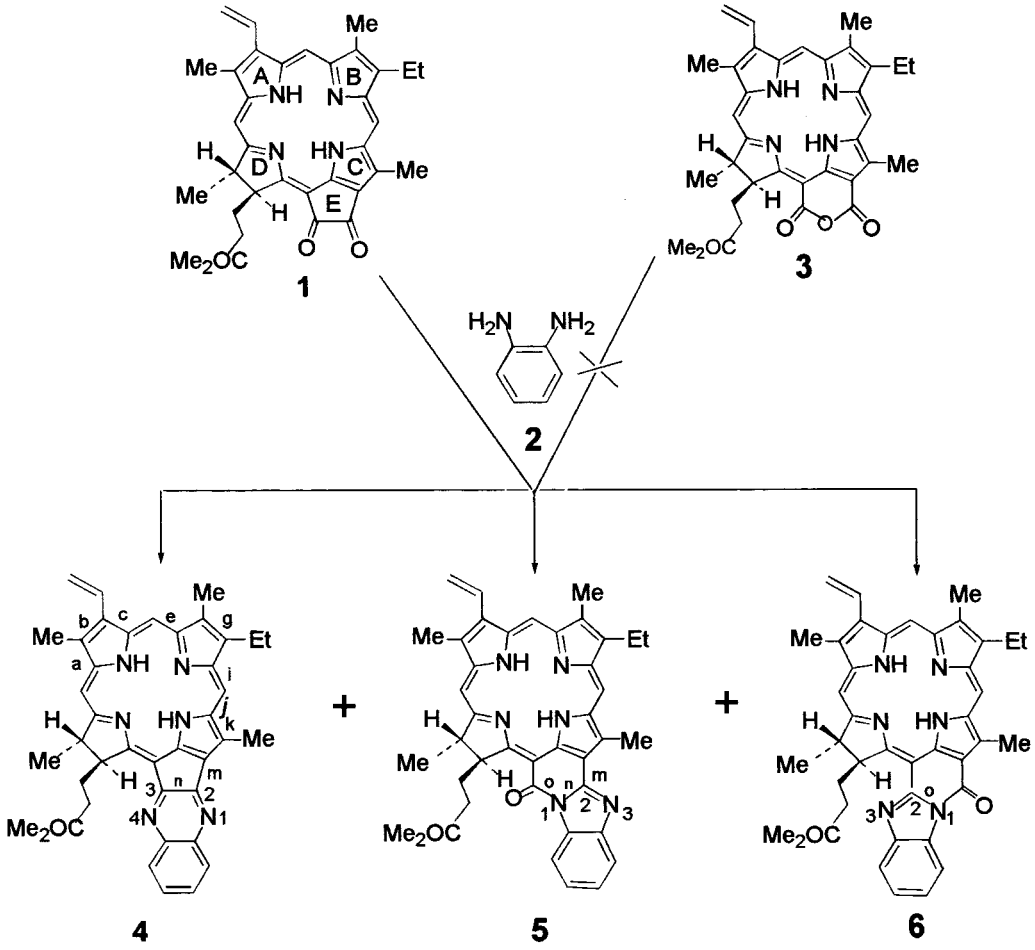

Scheme 1.

chlorins containing fused quinoxaline, benzimidazole and perimidine polyaromatic systems. The photophysical properties of some of these compounds are also discussed.

Results and Discussion

Chemistry

Quinoxaline condensation, a well-known reaction in organic chemistry has been successfully exploited in porphyrins for the preparation of quinoxalinoporphyrins,[14] extended at β-pyrrolic positions and porphyrinoids related to texaphyrins.[15] This chemistry provides an excellent approach for designing the extended porphyrin π-systems connected in a linear fashion.

In our approach to prepare photosensitizers with long wavelength absorption, methyl 13^2-oxopyropheophorbide *a* **1** was thought to be an ideal substrate for building chromophores with extended conjugation through an inherent five membered exocyclic ring (ring E). For preparing such novel structures, we selected a series of diamines such as **2**, **7**, **11**, **13**, **15**. These amines were reacted individually with dione **1**. In our initial attempts, the reaction conditions were optimized by using 1,2-phenylenediamine **2** as a substrate. Condensation of the chlorin **1** with **2** in pyridine in the presence of a catalytic amount of trifluoroacetic acid (TFA) afforded a mixture of three products. The least polar yellow–brown major band (55% yield) produced the required molecular ion (*m/z*: 635) and was assigned as the quinoxaleno[2,3-*n*]pheophorbide *a* methyl ester **4**. As expected, in chlorin **4**, the Soret band as well as the Q_y bands demonstrated significant red shifts and were observed at 438 and 708 nm respectively. The ^{1}H NMR spectrum of **4** showed distinctive low-field signals of quinoxaline ring hydrogens as two sets of multiplets at δ=7.64 and 8.03 ppm. As a result of extended conjugation, the resonances observed as singlets for 10- and 5-*meso* protons were found to be markedly shielded ($\Delta\delta$=−0.4 and −0.3 ppm) as compared to **1** due to increased ring current. On the other hand, the upfield shift for 17′a/17′b hydrogens of the propionic side chain ($\Delta\delta$=0.2 ppm) was attributed to their close proximity with the quinoxaline π-moiety.

The identification of the structure of two other chlorins (the most mobile green band and a polar red band) was intriguing. Both compounds exhibited even larger bathochromic shift for their Q_y-bands than did chlorin **4**, which suggested that these products have extended conjugation with a possibility of an additional electron-withdrawing functionality. Interestingly, the mass-spectra of both compounds gave a molecular ion peak (*m/z*) at 651.3 Daltons, indicating the presence of an extra oxygen

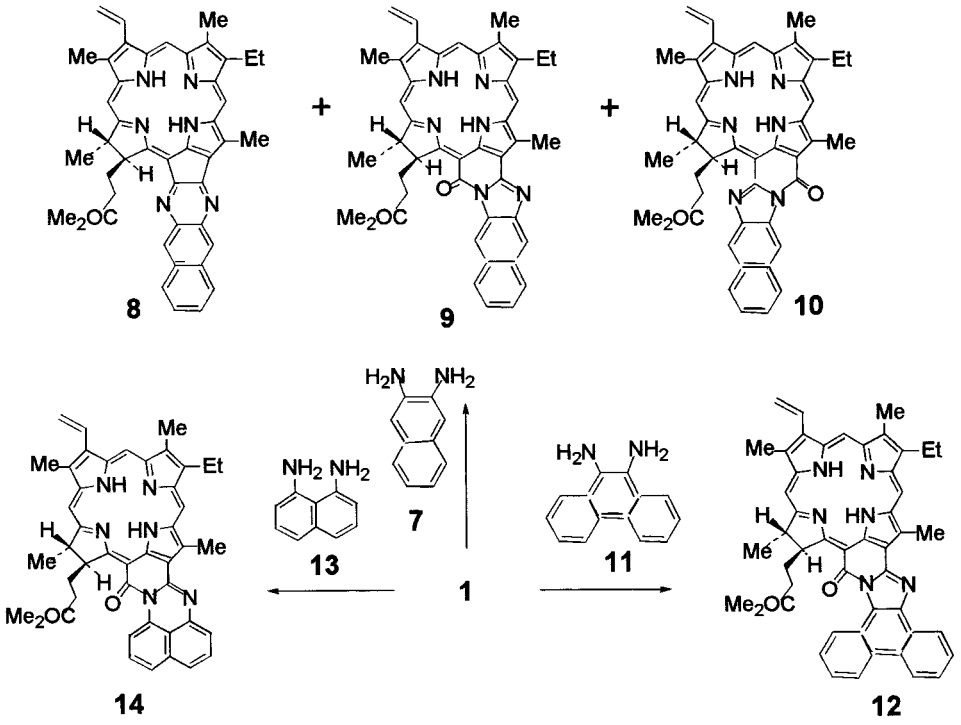

Scheme 2.

atom in these molecules than observed for the quinoxalino[1,2-*n*]pheophorbide *a* methyl ester **4**. Based on extensive ^{1}H NMR studies, we assigned their structures as annulated benzimidazo[1,2-*o*]purpurin-18 13^1-imino-13^2-imide methyl ester **6** for the minor product (green band, 5% yield) and an isomeric benzimidazolo[2,1-*n*]-derivative **5** for the major component (red band, 37% yield), respectively. These assignments were made on the basis of the characteristic chemical shifts observed for the proton at position-17 (17-H), located in close proximity to the benzimidazole system. Thus, compared to compound **5**, in which the 17-H was found at 5.49 ppm, chlorin **6** has more deshielded 17-H resonance and was appeared as a doublet of doublet (dd) at δ 5.74 ppm. Similar upfield effects of the 15^1-keto-/imine functions on the neighboring 17-H resonance were also observed for isomeric isoimide derivatives of purpurin-18.[7] Due to the presence of a keto-group, the resonances for the benzimidazole ring hydrogens were observed as three sets of multiplets, with the upfield shifted doublets of more closely located 8′-H at 8.87 for **5** and 8.62 ppm for chlorin **6** respectively. These assignments were further confirmed by a single crystal X-ray crystallography analysis (Scheme 1).

To investigate the stability of **4** and the mechanism of the formation of oxidized products, it was refluxed with pyridine for 3 h in the presence of TFA for an extended time and was found to be stable. These results concluded that the formation of benzimidazole derivatives might involve in situ autooxidation. The preferential formation of isomer **5** vs. **6** is possibly due to higher reactivity of 13^1-keto function[13] in chlorin **1** as well as due to less steric effect, being away from propionic ester functionality, to produce the corresponding Schiff base. This reaction was studied under variable reaction conditions and the intermediate Schiff base was found to be extremely sensitive to oxidation. The yields of the oxidation products **5** and **6** vary upon the reaction conditions used. In general, a large excess of TFA and higher temperature led to the preferential formation of oxidized products **5** and **6** up to 64 and 8% respectively. It is noteworthy to mention that our initial attempts to synthesize benzimidazole-annulated derivatives **5**,**6** via a direct condensation of purpurin-18 methyl ester **3** with 1,2 diaminobenzene **2** were unsuccessful, presumably due to low reactivity of conjugated anhydride ring.

This methodology was extended further for the preparation of a series of chlorins with various fused heterocyclic polyaromatic fragments by using several diamines as the building blocks. While the yields for compounds **8**–**10** were similar to **4**–**6**, condensation with diamine **11** resulted in the formation of the only phenanthroimidazo-annulated derivative **12** in low yield (13%), which can be attributed due to low reactivity of diamine **11**. Interestingly, reaction of diketone **1** with 1,8-diaminonaphthalene **13** produced only one product, which was identified as perimidino[2,1-*n*] derivative of purpurin-18 **14**. The 2D-ROESY ^{1}H NMR data of the reaction product did not show any through-space interactions of the naphthalene protons with the methylene protons of the propionic ester functionality, suggesting **14** as the only possible structure (Scheme 2).

We explored this methodology for the construction of laterally bridged pyropheophorbide *a* dimer. In this approach, diketochlorin **1** was condensed with 1,2,4,5-benzenetetramine tetrahydrochloride **15**. The best yield of dimer **16** (23%) was obtained by refluxing the reaction mixture in CH_2Cl_2 for 4 days with a catalytic amount of TFA under nitrogen atmosphere. As observed for the condensation with aromatic diamines, besides the expected

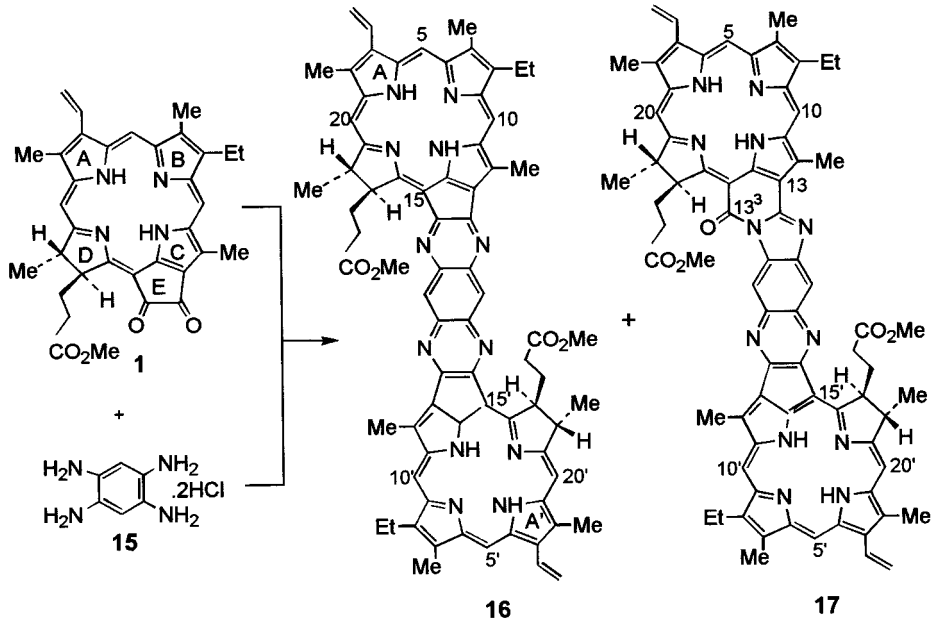

Scheme 3.

dimer **16** (*m/z* 1190), the oxidized benzimidazolo-annulated product **17** (yield: 8%) was also isolated (Scheme 3).

The ^{1}H NMR studies of the fused bis-chlorin suggested that in dimer **16** there is a diagonal symmetry between the pyrrolic rings A and A′ of chlorin units. A similar *trans*-diagonal arrangement of chromophores has been reported for the 13^1-conjugated bis-pyropheophorbide *a*, as a more favorable structure due to the steric hindrance of the propionic ester side chain present in ring D.[16] The ^{1}H NMR of dimer **17** supported this assignment, showing the distinctive singlet of equivalent hydrogen atoms of the bis-quinoxaline bridge at δ 7.89 ppm, and other unique characteristics. For example, compared to the parent compound **1**, the resonances for various protons generally appeared to be broader and the resonances representing the meso-protons as singlets showed a remarkable upfield shift (δ=0.8–1.2 ppm). All the resonances of the methyl protons were unusually collapsed into a sharp singlet observed at 3.62 ppm. Interestingly, similar dramatic changes have also been reported in the NMR spectra of certain chlorophyll enolates.[16] These similarities can be explained by the enolic characteristic of the 13^1-13^2 bound due to an electron delocalization effect. Extended conjugation of chlorin macrocycles in dimer **6** through the bis-pyrazine/benzene spacer showed a profound effect on the delocalization of the π-electrons. The large chemical shifts of meso-protons in the NMR spectrum also reflect a marked reduction of the ring current caused by electron delocalization and 'enolization increment'[17] effects.

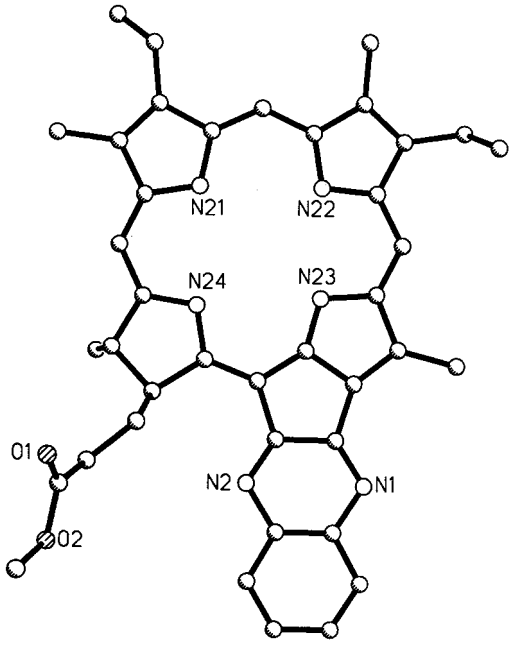

Figure 1. X-Ray crystal structure of chlorin **4**. Hydrogen atoms have been omitted for clarity; ellipsoides show 50% occupancy.

The structure for the unsymmetrical dimer **17** was confirmed by mass (*m/z* 1206) and NMR analyses.[1] In the ^{1}H NMR spectrum, as expected, the resonances of two different chlorin units were observed, which were most distinctive for the 17/17′ and 18/18′ protons. The position of the oxo-functionality at 13^3-position was assigned on the basis of the specific chemical shift of the 17-H at δ 6.74 observed for the related monomer chlorin **5** (confirmed by 2D ROESY NMR and X-ray studies). The electronic absorption spectrum of dimer **17** did not show the absorption peaks observed by the independent chlorin chromophores, but produced a single red-shifted Soret band at 459 nm and Q_y-band at 744 nm, which indicates that this unsymmetrical dimer is behaving as one large conjugated system.

Laterally bridged chlorins **16** and **17** are of special interest, because the related conjugated porphyrin arrays have received considerable attention as biomimetic models[18] for

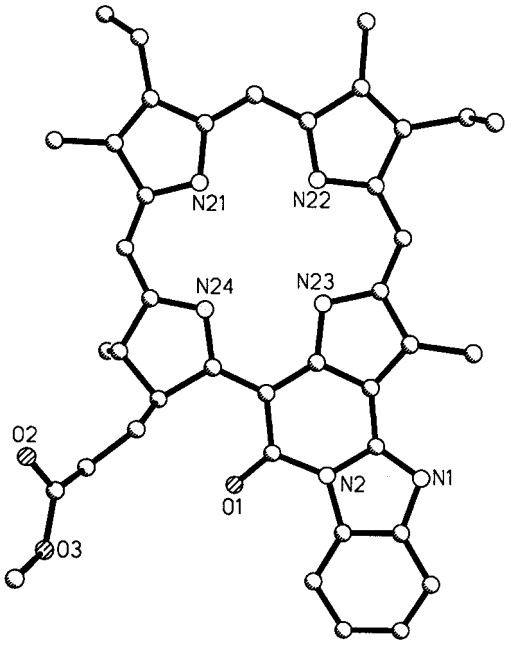

Figure 2. X-Ray crystal structure of chlorin **5**. Hydrogen atoms have been omitted for clarity; ellipsoides show 50% occupancy.

study of electron transfer processes.[19] Although porphyrins have proven to be valuable model compounds, we consider that conjugated chlorin dimers with defined geometry are a useful step towards more biologically relevant model systems.[20]

X-Ray crystallography and modeling studies

The molecular constitution of the compounds **4** (Fig. 1) and **5** (Fig. 2) was ascertained by single crystal X-ray structural analysis. The structures and the molecular packing of the two compounds are uneventful and typical for pheophorbide *a* derivatives. Both molecules exhibit a more or less planar macrocycle (deviations of the 24 macrocycle atoms from their least-squares-plane are 0.05 Å for **4** and 0.07 Å for **5** respectively). Some deviations from planarity are observed for the C_b positions of the reduced pyrrole ring. Both compounds exhibit a stacked arrangement of the molecules in the crystal and small interplanar separations (3.14 Å). However, there is almost no overlap between individual macrocycles and/or the aromatic substituents at ring C. Thus, no effective π-stacking is observed.

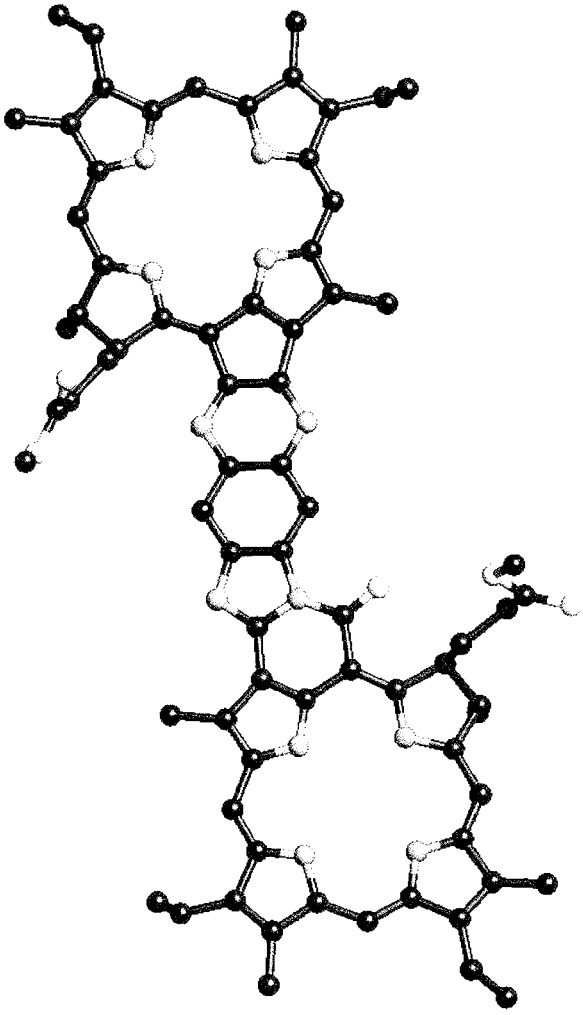

Figure 3. Molecular mechanics energy optimized model structure of dimer **17** constructed from crystal structures of the corresponding monomers.

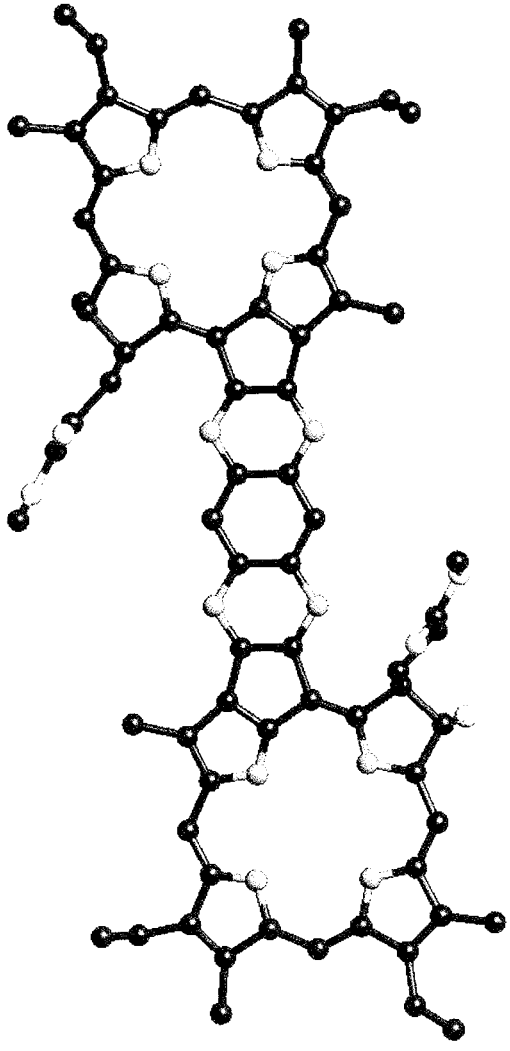

Figure 4. Molecular mechanics energy optimized structure of dimer **16** constructed from crystal structures of the corresponding monomers.

Table 1. Absorption properties of chlorins as momomers and dimers (in benzene)

Compound	Absorption λ_{max} (nm) (ϵ [10^5 M^{-1} cm^{-1}])			
	S_1	S_2	Q_x	Q_y
1	390 (0.51)	420 (0.46)	516 (0.07)	678 (0.31)
4	363 (0.49)	438 (1.39)	528 (0.26)	708 (0.46)
8	369 (0.56)	456 (1.42)	537 (0.29)	712 (0.51)
3	363 (0.49)	412 (1.25)	548 (0.26)	699 (0.49)
5	382 (0.49)	426 (1.29)	558 (0.34)	729 (0.61)
9	384 (0.48)	428 (1.34)	567 (0.37)	735 (0.67)
12	389 (0.53)	429 (1.43)	568 (0.38)	744 (0.69)
6	395 (0.76)	420 (1.14)	591 (0.38)	714 (0.68)
10	399 (0.78)	423 (1.23)	594 (0.39)	720 (0.71)
14	365 (0.41)	414 (1.32)	600 (0.12)	720 (0.81)
16	399 (0.82)	498 (1.29)	549 (0.41)	720 (0.71)
17	378 (0.58)	459 (1.49)	567 (0.28)	744 (0.65)

The energy optimized structures for the dimers are obtained on the basis of the crystal data of the monomeric units and are shown in Figs. 3 and 4. The large conjugated plane systems are measured approximately as a 9 Å×23 Å rectangular shape. The energy optimization left it essentially planner with the root mean square distance of atoms from the plane to be 0.17 and 0.12 Å for homo- and heterodimer respectively. Although there is a difference in their sizes as measured by the meso carbon to meso carbon distances: C5–C5′ distance is 23.3 Å for homodimer and 23.5 Å for heterodimer while 10.0 and 10.01 Å are obtained for C15–C15′ distance for homo- and heterodimer respectively.

Photophysical properties

These novel chlorins containing fused heterocyclic polyaromatic fragments and dimers showed some unique optical properties. On the basis of the presence of the parent chromophore system,[21,22] they were divided into three groups. In each series these compounds demonstrated bathochromic shifts of their Soret and Q_y-bands accompanied by an hyperchromic effect compared to non-extended chlorins **1** and purpurin methyl ester **3** (Table 1). For example, compared to the parent molecule, chlorin **4** had an 18 nm red shift for the Soret band, while compound **8** showed an even larger bathochromic effect ($\Delta\lambda$=36 nm) as a result of their increased π-conjugation. Similar relationships were also demonstrated for annulated purpurin-18 derivatives. It was interesting to observe that all quinoxaline derivatives **4** and **8**, as well as the parent chromophore **1**, have a minor absorption band Q_x at 520–530 nm, which is responsible for its yellowish color in solution. On the other hand, benzimidazole derivatives **5**, **9** and **12** exhibited purpurin-18-type absorption around 550 nm, providing a red color, while isomers **6** and **10** also showed absorption near 600 nm and were blue–green in color respectively. Unlike other chlorins, compound **12** showed a distinctive absorption of the dibenzo[*f*,*h*]quinoxaline polyaromatic fragment at 330 nm. Absorption spectra of laterally bridged dimers **16** and **17** have some similarity to related monoannulated chlorins **5** and **6** demonstrating both hyperchromic and bathochromic effect as well as some unique characteristics. For example, the UV/vis spectrum of dimer **16** has a characteristic split and a strongly red-shifted Soret band at 498 nm. This characteristic was found to be analogous to the absorption spectra reported for pheophytin *a* enolates,[13] which also exhibit similar splitting and a red shift of their Soret bands. This unique characteristic could be due to the extensive intramolecular π-electron distribution caused by the 13^1-13^2 carbon–carbon bond in isocyclic rings E and E′ which have typical enolic double bond characteristics.[17] Interestingly, the electronic absorption spectrum of dimer **17** did not show the absorption peaks observed for the two independent chlorin chromophores, but produced a single red shifted Soret band at 459 nm and Q_y-band at 744 nm, which indicates that the unsymmetrical dimer **17** is behaving as one large conjugated system.

Table 2. Emission properties of monomers and dimers (in benzene)

Compound	Excitation peak (λ_{max}) (nm)	Emission (λ_{max}) (nm)	ϕ_f	τ_f (ns)
4	438	719	0.076	4.09
5	426	742	0.06	3.52
6	420	744	0.16	4.8
14	415	–	<0.001	–
16	400	725	0.067	4.3
17	459	750	0.057	2.5

The emission properties of the chlorin derivatives are summarized in Table 2. Compounds **4**–**6**, **16** and **17** show weak fluorescence with (ϕ_f~0.08–0.16) and lifetimes ranging from 2–5 ns. Compound **14** did not show any measurable fluorescence.

Nanosecond laser flash photolysis of all compounds except **14**, showed moderately strong transient absorption with bleaching in the regions where they absorb strongly in the ground state. The time resolved transient absorption spectrum recorded for **6** is shown in Fig. 5.

The transient absorption which is formed within the laser pulse decays by a first order process. The decay of the transient leads to a recovery of the ground state absorption indicating negligible formation of any permanent photoproducts (Inset Fig. 5). Similar behavior was observed for all the other compounds studied. The transient absorption observed for these compounds could be attributed to the triplet state by energy transfer to β-carotene. Quenching of the transient species led to the formation of β-carotene triplet. Since the intersystem crossing efficiency of the β-carotene triplet is negligible, formation of its triplet state confirms the triplet nature of the transient species formed on excitation of compounds **4**–**6**, **16** and **17**.

The triplet yields (ϕ_T) of the compounds in toluene were measured by energy transfer to β-carotene, using the 355 nm excitation.[23,24] Optically matched solutions of the chlorin derivatives in toluene and benzophenone in benzene were mixed with a known volume of a 1 mM solution of β-carotene in benzene. In the case of benzophenone, benzene had to be used instead of toluene as solvent in order to circumvent the problem of hydrogen atom abstraction by the triplet state of benzophenone. It was however ascertained that the behavior of the triplet state of the chlorin derivatives were the same, both in benzene and in toluene. The transient absorbance of β-carotene at 540 nm was monitored and the triplet quantum yields were

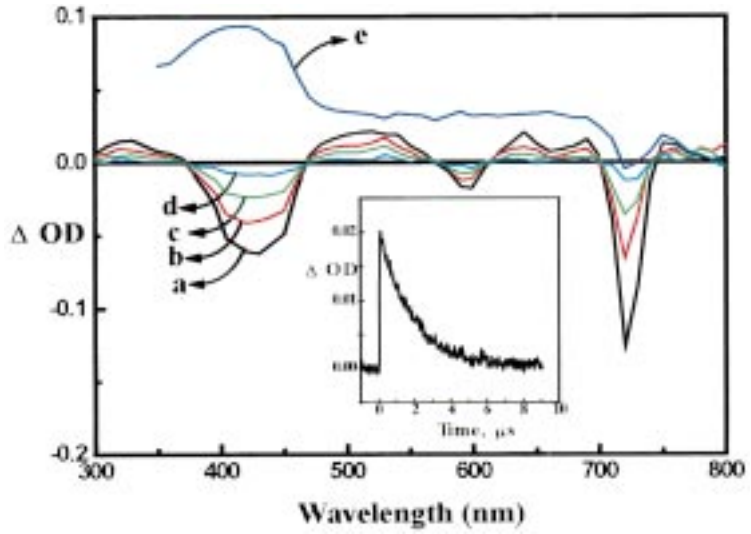

Figure 5. Transient absorption spectra at different time intervals recorded following laser pulse (355 nm) excitation of **5** in toluene (a) 1.7×10^{-7}; (b) 1.01×10^{-6}; (c) 2.01×10^{-6}; (d) 4.01×10^{-6} s; (e) Transient absorption spectrum of compound **5** immediately after the laser pulse corrected for the ground state absorption. Inset shows the decay of the transient absorption at 520 nm.

Table 3. Triplet excited state properties of monomers and dimers (in benzene)

Compound	λ_{max} (ΔOD)	τ_T (μs)	ϕ_T	$\phi_{\Delta S}$
4	480 (0.045)	1.09	0.58	0.56
5	590 (0.103)	1.4	0.56	0.51
6	520 (0.021)	1.9	0.39	0.36
14		–	<0.01	–
16	580 (0.006)	1.0	0.47	0.41
17	600 (0.008)	4.5	0.42	0.32

measured using the following expression:

$$\phi_T^S = \phi_T^R\left(\frac{\Delta A^S}{\Delta A^R}\right)\left(\frac{k_{obs}^S}{k_{obs}^S - k_o^S}\right)\left(\frac{k_{obs}^R - k_o^R}{k_{obs}^R}\right)$$

where ϕ_T, ΔA, k_{obs} and k_o are the triplet yield, the plateau absorbance following the completion of sensitized triplet formation, the pseudo first order rate constant for growth of the β-carotene triplet sensitized by chlorin or benzophenone, and the rate constant for decay of a triplet in the absence of β-carotene, respectively. S and R denote sample and reference.

The absorption maxima, lifetimes and quantum yields of the triplet states of all the compounds are shown in Table 3.

The triplet yields are fairly large for all compounds except for the derivative **14**. As in the case of fluorescence, the triplet yield of **14** was also negligible, indicating that the excited state of the compound undergoes very rapid decay through a non-radiative pathway to the ground state. The quantum yields of singlet oxygen formation (Table 3) were determined by comparing the efficiency of photooxidation

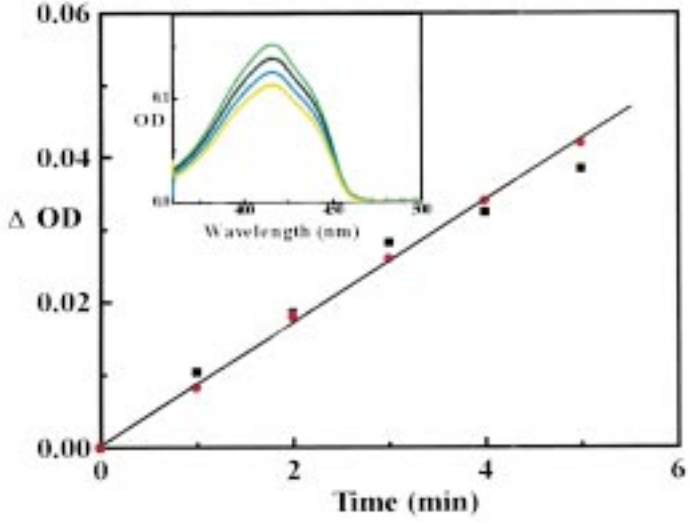

Figure 6. Plot of absorption change of 1,3-diphenylisobenzofuran at 410 nm vs. irradiation time (λ_{irr}=560 nm) in the presence of compound **1** (-●-●-) in toluene and Rose Bengal (-■-■-) as the standard in methanol. Inset shows the absorption spectra of DPBF at various irradiation time intervals in presence of compound **1**.

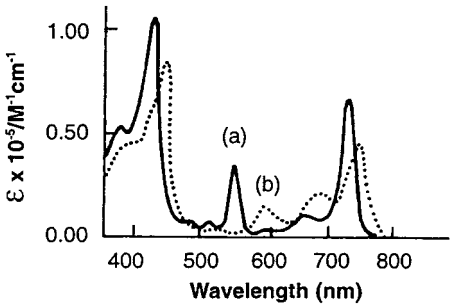

Figure 7. Electronic absorption spectra (in CH_2Cl_2) of (a) chlorin **5** and (b) its enolate.

Table 4. Absorption properties of lithium enolates of chlorins as monomers and dimers[1]

Compound	Absorption λmax (nm) (ε [10^5 M^{-1} cm^{-1}])			
	S_1	S_2	Q_x	Q_y
4 (LiOH/THF)	414 (0.57)	438 (1.21)	576 (0.12)	738 (0.39)
5 (LiOH/THF)	393 (0.48)	426 (0.89)	693 (0.21)	744 (0.46)
6 (LiOH/THF)	412 (0.72)	453 (1.26)	633 (0.25)	731 (0.41)
14 (LiOH/THF)	405 (0.56)	441 (0.94)	612 (0.23)	723 (0.89)
16 (LiOH/THF)	423 (0.79)	558 (1.12)	636 (0.49)	774 (0.51)
17 (LiOH/THF)	375 (0.59)	501 (1.36)	609 (0.29)	774 (0.69)

of DPBF[25] by the compound of interest, to that of a standard, namely, Rose Bengal ($\phi_{\Delta S}$=0.46).[26] DPBF was used as it absorbs in a region where the chlorin derivatives absorb weakly and it rapidly reacts with singlet oxygen to form a colorless product.[27,28] Solutions were irradiated at 560 nm using a 450 W output of Xenon arc lamp. A monochromator (SPEX 1681 0.22 m) was used to select the irradiation wavelength. The quantum yields were measured in optically dilute solutions (OD~0.1), using the following expressions:

$$\phi_{\Delta S} = \phi_{\Delta R} \times \frac{m_S}{m_R} \times \frac{(1 - 10^{-OD})_R}{(1 - 10^{-OD})_S}$$

where S and R refer to sample and reference, m is the slope of a plot of change in DPBF absorbance at 410 nm with irradiation time (Fig. 6, $1-10^{-OD}$ is the absorbance correction factor at the irradiation wavelength.

The quantum yields of singlet oxygen, measured using the steady-state technique, are also listed in Table 3. The triplet and singlet oxygen yields are the same within the experimental error, indicating efficient energy transfer from the triplet excited state to oxygen.

Vinylogous-type enolization

Recently we have shown that introduction of oxo-functionalities into isocyclic ring E strongly influences the neighboring 12-methyl substituent, which can undergo vinylogous enolization upon reacting with LiOH. These enolates have characteristic UV-visible spectra with broad, split and red shifted Soret bands. Because both parent 13^2-oxopyropheophorbide *a* **1** and purpurin-18 methyl ester **3** exhibited vinylogous enolization of the 12-methyl group, we had expected to observe similar characteristics for annulated chlorins and the related dimeric systems, and indeed all new chromophores produced a distinctive pattern of 12-methyl enolization.

Thus, compared to parent compounds **4**–**6**, **14**, **16** and **17**, the UV-visible spectra of their corresponding lithium enolates (Fig. 7) exhibited a significant red shift of their Soret bands (Table 4), the maximum shift being observed for dimer **16** ($\Delta\lambda$=60 nm), with a small decrease in the intensity (hypsochromic effect). In contrast, the Q_x-bands of enolates demonstrated significant increase in intensity and a marked bathochromic shift in the range $\Delta\lambda$=36–51 nm, thus making a distinctive change in their colors. Enolization also affected the Q_y absorptions of annulated chlorins **4**–**6**, and the dimers **16**,**17**, causing a red shift with a small hypsochromic effect. Compound **14**'s enolate Q_y-band was an anomaly, exhibiting a hyperchromic effect, but no bathochromic shift.

Vinylogous enolization of polyaromatic annulated chlorins is a reversible process, and on treatment with acid, the UV-visible spectra of lithium enolates reverted back to those corresponding to the parent compounds (Scheme 4).

Conclusion

A first synthesis of a series of chlorins with fused quinoxaline and benzimidazole-aromatic rings has been accomplished by condensation of 13^2-oxopyropheophorbide *a* with diamino aromatic compounds under acid-catalyzed conditions. These compounds demonstrated hyperchromic and bathochromic effects on their Soret and Q-absorption bands due to extended conjugation. This methodology was also used for the preparation of a laterally bridged bis-quinoxaline pheophorbide *a* dimer. Spectroscopic data of novel conjugated dimers show a significant perturbation of the extended bis-chlorin π-system in a coplanar arrangement. The synthetic approach developed here provides great potential for designing novel chromophores with extended π-conjugation and building molecular photonic devices, e.g. chlorin–porphyrin, chlorin–bacteriochlorin, bacteriochlorin–bacteriochlorin fused heterosystems.

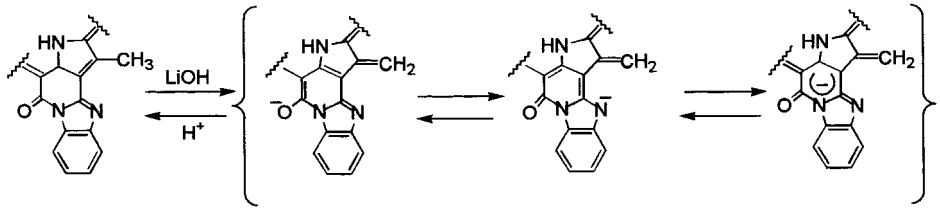

Scheme 4.

Chlorins **4** and **5** displayed high quantum yields of singlet oxygen producing efficiency (Table 1), which along with their red shifted prominent absorotions (Q_y band) make them attractive candidates as photosensitizers for PDT. The in vivo biological studies with these compounds are currently in progress and will be published elsewhere.

Experimental

Melting points were determined on a melting point apparatus and are uncorrected. NMR spectra were recorded on Brucker 400 and 600 MHz NMR spectrometers and are expressed in δ ppm. Mass spectral data were received from University of Michigan, East Lansing. Diphenylisobenzofuran (DPBF) and benzophenone were obtained from Aldrich and 3,3′-diethyloxatricarbocyanine iodide (DOTCI) was obtained from Exciton Inc. All photophysical experiments were carried out using spectroscopic grade solvents.

Absorption spectra were recorded on a Shimadzu UV-3101 PC UV–VIS NIR spectrophotometer or on a Genesis 5 spectrophotometer. Emission spectra were recorded on a Spex-Fluorolog F112X spectrofluorimeter. The emission spectra were corrected by the program supplied by the manufacturer. Quantum yield of fluorescence (ϕ_f) was determined by the relative method using optically dilute solution of DOTCI in ethanol (ϕ_f=0.49)[29] as reference. The measurements were performed on optically matched solutions and the quantum yields were corrected for the refractive index of solvents. Fluorescence lifetimes were determined using Edinburgh Instruments FL 900 CD single photon counting system.

The laser flash photolysis experiments were carried out using the third harmonic (355 mm) of a Nd:YAG laser GCR-12 series, Quanta Ray of 10 ns pulse width. The kinetic absorption spectrophotometer used to detect the optical density changes after laser excitation (LKS-20, Applied Photophysics) has been described earlier.[30]

General method of synthesis

To a solution of methyl 13^2-oxopyropheophorbide *a* **1** (56 mg, 0.1 mM) in pyridine (50 ml), containing TFA (0.1 ml), diamine (**2**, **7**, **11**, **13**) (100 mg) was added individually and the reaction mixture stirred at 50°C for 2 h. The mixture was poured into water (500 ml), the products were extracted with CH_2Cl_2 (3×50 ml). The combined extracts were washed with 1% aqueous acetic acid (2×500 ml), then with water (2×300 ml), dried over sodium sulfate, and the solvent removed under reduced pressure. The residue was chromatographed on a silica column eluting with 1% acetone/CH_2Cl_2 in several fractions, which were purified by preparative TLC. Recrystallization from CH_2Cl_2/methanol gave chlorins **4**–**14** depending on the diamine used.

All conjugated chlorins and dimers **16**,**17** had melting points above 270°C with decomposition, and were not corrected.

Quinoxalino[2,3-*n*]deoxopyropheophorbide *a* methyl ester (4) (35 mg, 55%); UV/vis (CH_2Cl_2): $\lambda_{max}(\epsilon)$=438 (120,000), 528 (16,000), 657 (4500), 708 nm (45,700): ^{1}H NMR ($CDCl_3$): δ=−0.92 (br s, 2H, 2×NH), 1.69 (t, *J*=7.5 Hz, 2H, 8^2-CH_3), 1.88 (d, *J*=8 Hz, 3H, 18-CH_3), 2.41 (m, 1H, 17^2_b-H), 2.49 (m, 1H, $17^2_{b'}$-H), 2.75 (m, 1H, $17^1_{a'}$-H), 2.92 (m, 1H, 17^1_a-H), 3.24 (s, 3H, 7-CH_3), 3.39 (s, 3H, 2-CH_3), 3.68 (s, 3H, CO_2CH_3), 3.72 (q, *J*=7.5 Hz, 2H, 8^1-CH_2), 3.79 (s, 3H, 12-CH_3), 4.51 (q, *J*=8 Hz, 1H, 18-H), 5.19 (dd, *J*=4.5 Hz, 1.5 Hz, 1H, 17-H), 6.18 (d, *J*=11.3 Hz, 1H, $3^2_{b'}$-H), 6.22 (d, *J*=17.5 Hz, 1H, 3^2_b-H), 7.64 (m, 2H, quinoxaline-H), 7.94 (dd, *J*=11.3 Hz, 17.5 Hz, 1H, 3^1-H), 8.03 (m, 2H, quinoxaline-H), 8.57 (s, 1H, 20-H), 9.39 (s, 1H, 5-H), 9.46 (s, 1H, 10-H); MS: *m*/*z* (%)=635.4 (MH^+, 100%), 547.4 (23%); HRMS (EI): calcd for $C_{40}H_{38}N_6O_2$: *m*/*z* 635.3086; found: 635.3163.

Benzimidazolo[2,1-*n*]purpurin-18 13^1-imino-13^2-imide methyl ester (5) (24 mg, 37%); UV/vis (CH_2Cl_2): $\lambda_{max}(\epsilon)$=426 (120,000), 558 (16,500), 677 (4500), 729 nm (49,500): ^{1}H NMR ($CDCl_3$): δ=0.12 (br s, 2H, 2×NH), 1.64 (t, *J*=7.5 Hz, 2H, 8^2-CH_3), 1.85 (d, *J*=8 Hz, 3H, 18-CH_3), 2.04 (m, 1H, 17^2_b-H), 2.44 (m, 2H, $17^2_{b'}$,$17^1_{a'}$-H), 2.81 (m, 1H, 17^1_a-H), 3.14 (s, 3H, 7-CH_3), 3.32 (s, 3H, 2-CH_3), 3.67 (s, 3H, CO_2CH_3), 3.68 (q, *J*=7.5 Hz, 2H, 8^1-CH_2), 3.78 (s, 3H, 12-CH_3), 4.43 (q, *J*=8 Hz, 1H, 18-H), 5.49 (dd, *J*=4.5, 1.5 Hz, 1H, 17-H), 6.22 (d, *J*=11.7 Hz, 1H, $3^2_{b'}$-H), 6.24 (d, *J*=17.9 Hz, 1H, 3^2_b-H),), 7.48 (m, 2H, benzimidazole-H), 7.89 (dd, *J*=11.7 Hz, 17.9 Hz, 1H, 3^1-H), 7.94 (m, 1H, benzimidazole-H), 8.57 (s, 1H, 20-H), 8.87 (m, 1H, benzimidazole-H), 9.32 (s, 1H, 10-H), 9.41 (s, 1H, 10-H); MS: *m*/*z* (%)=651.4 (MH^+, 100%), 563.3 (19%); HRMS (EI): calcd for $C_{40}H_{38}N_6O_3$: *m*/*z* 651.3036; found: 651.3163.

Benzimidazolo[1,2-*o*]purpurin-18 13^3-imino-13^2-imide methyl ester (6) (3 mg, 5%); UV/vis (CH_2Cl_2): $\lambda_{max}(\epsilon)$=381 (93,000), 426 (120,000), 447 (91,500), 588 (16,000), 675 (4500), 714 nm (49,500): ^{1}H NMR ($CDCl_3$): δ=0.22 (br s, H, NH), 0.36 (br s, H, NH), 1.66 (t, *J*=7.5 Hz, 2H, 8^2-CH_3), 1.83 (d, *J*=8 Hz, 3H, 18-CH_3), 2.01 (m, 1H, 17^2_b-H), 2.54 (m, 2H, $17^2_{b'}$,$17^1_{a'}$-H), 2.86 (m, 1H, 17^1_a-H), 3.08 (s, 3H, 7-CH_3), 3.36 (s, 3H, 2-CH_3), 3.63 (q, *J*=7.5 Hz, 2H, 8^1-CH_2), 3.67 (s, 3H, CO_2CH_3), 3.78 (s, 3H, 12-CH_3), 4.41 (q, *J*=8 Hz, 1H, 18-H), 5.74 (dd, *J*=4.5, 1.5 Hz, 1H, 17-H), 6.20 (d, *J*=11.4 Hz, 1H, $3^2_{b'}$-H), 6.24 (d, *J*=18.0 Hz, 1H, 3^2_b-H),), 7.46 (m, 2H, benzimidazole-H), 7.87 (dd, *J*=11.4, 18.0 Hz, 1H, 3^1-H), 7.91 (m, 1H, benzimidazole-H), 8.52 (s, 1H, 20-H), 8.62 (m, 1H, benzimidazole-H), 9.22 (s, 1H, 5-H), 9.38 (s, 1H, 10-H); MS: *m*/*z* (%)=651.4 (MH^+, 100%), 563.3 (19%); HRMS (EI): calcd for $C_{40}H_{38}N_6O_3$: *m*/*z* 651.3036; found: 651.3089.

Benzo[*g*′]quinoxalino[2,3-*n*]pheophorbide *a* methyl ester (8) (36 mg, 52%); UV/vis (CH_2Cl_2): $\lambda_{max}(\epsilon)$=456 (120,000), 528 (16,000), 657 (4500), 720 nm (45,700): ^{1}H NMR ($CDCl_3$): δ=−1.46 (br s, 2H, 2×NH), 1.63 (t, *J*=7.5 Hz, 2H, 8^2-CH_3), 1.98 (d, *J*=8 Hz, 3H, 18-CH_3), 2.41 (m, 1H, 17^2_b-H), 2.46 (m, 1H, $17^2_{b'}$-H), 2.78 (m, 1H, $17^1_{a'}$-H), 2.92 (m, 1H, 17^1_a-H), 3.12 (s, 3H, 7-CH_3), 3.39 (s, 3H, 2-CH_3), 3.46 (s, 3H, 12-CH_3), 3.51 (q, *J*=7.5 Hz, 2H, 8^1-CH_2), 3.68 (s, 3H, CO_2CH_3), 4.53 (q, *J*=8 Hz, 1H, 18-H),

5.22 (dd, J=4.5, 1.5 Hz, 1H, 17-H), 6.19 (d, J=11.5 Hz, 1H, $3^2_{b'}$-H), 6.23 (d, J=17.2 Hz, 1H, 3^2_b-H),), 7.32 (m, 2H, naphthalene-H), 7.88 (dd, 2H, naphthalene-H), 7.92 (dd, J=11.5, 17.2 Hz, 1H, 3^1-H), 8.12 (s, H, naphthalene-H), 8.28 (s, H, naphthalene-H), 8.59 (s, 1H, 20-H), 9.15 (s, 1H, 5-H), 9.43 (s, 1H, 10-H); MS: m/z (%)=685.6 (MH^+, 100%), 596.9 (16%); HRMS (EI): calcd for $C_{44}H_{40}N_6O_2$: m/z 685.3243; found: 685.3307.

Benzo[*f′*]benzimidazolo[2,1-*n*]purpurin-18 13^1-imino-13^2-imide methyl ester (9) (25 mg; 35%), UV/vis (CH_2Cl_2): $\lambda_{max}(\epsilon)$=426 (120,000), 558 (16,000), 677 (4500), 729 nm (49,500): ^{1}H NMR ($CDCl_3$): −0.22 (br s, 2H, 2×NH), 1.64 (t, J=7.5 Hz, 2H, 8^2-CH_3), 1.85 (d, J=8 Hz, 3H, 18-CH_3), 2.04 (m, 1H, 17^2_b-H), 2.44 (m, 1H, $17^2_{b'}$-H), 2.49 (m, 1H, $17^1_{a'}$-H), 2.81 (m, 1H, 17^1_a-H), 3.14 (s, 3H, 7-CH_3), 3.32 (s, 3H, 2-CH_3), 3.67 (s, 3H, CO_2CH_3), 3.68 (q, J=7.5 Hz, 2H, 8^1-CH_2), 3.78 (s, 3H, 12-CH_3), 4.43 (q, J=8 Hz, 1H, 18-H), 5.49 (dd, J=4.5, 1.5 Hz, 1H, 17-H), 6.12 (d, J=11.5 Hz, 1H, $3^1_{b'}$-H), 6.15 (d, J=17.5 Hz, 1H, 3^2_b-H),), 7.28 (m, 2H, naphthalene-H), 7.87 (m, 2H, naphthalene-H), 7.89 (dd, J=11.5, 17.5 Hz, 1H, 3^1-H), 7.96 (s, 1H, naphthalene-H), 8.54 (s, 1H, 20-H), 8.83 (s, 1H, naphthalene-H), 9.54 (s, 1H, 5-H), 9.55 (s, 1H, 10-H). MS: m/z (%)=701.4 (MH^+, 100%), 584.9 (12%); HRMS (EI): calcd for $C_{44}H_{40}N_6O_3$: m/z 701.3193; found: 701.3262.

Benzo[*g′*]benzimidazolo[1,2-*o*]purpurin-18 13^3-imino-13^2-imide methyl ester (10) (4 mg, 6%); UV/vis (CH_2Cl_2): $\lambda_{max}(\epsilon)$=381 (93,000), 426 (120,000), 447 (91,500), 588 (16,000), 675 (4500), 714 nm (49,500): ^{1}H NMR ($CDCl_3$): δ=0.12 (br s, H, NH), 0.16 (br s, H, NH), 1.67 (t, J=7.5 Hz, 2H, 8^2-CH_3), 1.88 (d, J=8 Hz, 3H, 18-CH_3), 2.23 (m, 1H, 17^2_b-H), 2.54 (m, 2H, $17^2_{b'}$,$17^1_{a'}$-H), 2.89 (m, 1H, 17^1_a-H), 3.08 (s, 3H, 7-CH_3), 3.38 (s, 3H, 2-CH_3), 3.65 (q, J=7.5 Hz, 2H, 8^1-CH_2), 3.67 (s, 3H, CO_2CH_3), 3.78 (s, 3H, 12-CH_3), 4.45 (q, J=8 Hz, 1H, 18-H), 5.84 (dd, J=4.5, 1.5 Hz, 1H, 17-H), 6.20 (d, J=11.5 Hz, 1H, 3^2_a-H), 6.23 (d, J=18.1 Hz, 1H, 3^2_b-H), 7.39 (m, 2H, naphthalene-H), 7.89 (dd, J=11.5, 18.1 Hz, 1H, 3^1-H), 7.91 (m, 2H, naphthalene-H), 8.19 (s, 1H, naphthalene-H), 8.52 (s, 1H, 20-H), 8.79 (s, 1H, naphthalene-H), 9.22 (s, 1H, 5-H), 9.39 (s, 1H, 10-H);. MS: m/z (%)=701.4 (MH^+, 100%), 684.9 (21%); HRMS (EI): calcd for $C_{44}H_{40}N_6O_3$: m/z 701.3193; found: 701.3205.

Phenanthro[9,10-*d′*]imidazolo[2,1-*n*]purpurin-18 13^3-imino-13^2-imide methyl ester (12) (7 mg, 9%); UV/vis (CH_2Cl_2): $\lambda_{max}(\epsilon)$=381 (93,000), 426 (120,000), 447 (91,500), 588 (16,000), 675 (4500), 714 nm (49,500): ^{1}H NMR ($CDCl_3$): δ=−1.12 (br s, H, NH), −1.03 (br s, H, NH), 1.38 (t, J=7.5 Hz, 2H, 8^2-CH_3), 1.68 (d, J=8 Hz, 3H, 18-CH_3), 1.93 (m, 1H, 17^1_b-H), 2.24 (m, H, $17^2_{b'}$-H), 2.34 (m, H, $17^1_{a'}$-H), 2.49 (m, 1H, 17^1_a-CH_2), 2.78 (s, 3H, 7-CH_3), 3.18 (s, 3H, 2-CH_3), 3.35 (q, J=7.5 Hz, 2H, 8^1-CH_2), 3.38 (s, 3H, 12-CH_3), 3.60 (s, 3H, CO_2CH_3), 4.23 (q, J=8 Hz, 1H, 18-H), 5.34 (dd, J=4.5, 1.5 Hz, 1H, 17-H), 6.01 (d, J=11.6 Hz, 1H, $3^2_{b'}$-H), 6.03 (d, J=17.6 Hz, 1H, 3^2_b-H), 6.97 (m, 1H, phenanthrene-H), 7.17 (m, 3H, phenanthrene-H), 7.28 (m, 1H, phenanthrene -H), 7.69 (dd, J=11.6, 17.6 Hz, 1H, 3^1-H), 8.49 (m, 1H, phenanthrene-H), 8.50 (s, 1H, 20-H), 9.12 (s, 1H, 5-H), 9.13 (s, 1H, 10-H); MS: m/z (%)=751.4 (MH^+, 100%), 636.5 (12%); HRMS (EI): calcd for $C_{48}H_{42}N_6O_3$: m/z 751.3350; found: 751.3374.

Perimidino[2,1-*n*]purpurin-18 13^3-imino-13^2-imide methyl ester (14) (48 mg; 69%), UV/vis (CH_2Cl_2): $\lambda_{max}(\epsilon)$=381 (93,000), 426 (120,000), 447 (91,500), 588 (16,000), 675 (4500), 714 nm (49,500): ^{1}H NMR ($CDCl_3$): δ=−1.12 (br s, H, NH), −1.03 (br s, H, NH), 1.38 (t, J=7.5 Hz, 2H, 8^2-CH_3), 1.68 (d, J=8 Hz, 3H, 18-CH_3), 1.93 (m, 1H, 17^2_b-H), 2.24 (m, H, $17^2_{b'}$-H), 2.34 (m, H, $17^1_{a'}$-H), 2.49 (m, 1H, 17^1_a-H), 2.78 (s, 3H, 7-CH_3), 3.18 (s, 3H, 2-CH_3), 3.35 (q, J=7.5 Hz, 2H, 8^1-CH_2), 3.38 (s, 3H, 12-CH_3), 3.60 (s, 3H, CO_2CH_3), 4.23 (q, J=8 Hz, 1H, 18-H), 5.34 (dd, J=4.5, 1.5 Hz, 1H, 17-H), 6.01 (d, J=11.5 Hz, 1H, $3^2_{b'}$-H), 6.03 (d, J=18.4 Hz, 1H, 3^2_b-H), 6.97 (m, 1H, naphthalene-H), 7.17 (m, 3H, naphthalene-H), 7.28 (m, 1H, naphthalene-H), 7.69 (dd, J=11.5, 18.4 Hz, 1H, 3^1-H), 8.49 (m, 1H, naphthalene-H), 8.50 (s, 1H, 20-H), 9.12 (s, 1H, 5-H), 9.13 (s, 1H, 10-H);.); MS: m/z (%)=701.4 (MH^+, 100%), 612.8 (36%); HRMS (EI): calcd for $C_{44}H_{40}N_6O_3$: m/z 701.3193; found: 701.3219.

Synthesis of laterally conjugated dimers

To a solution of methyl 13^2-oxopyropheophorbide *a* **1** (56 mg, 0.1 mM) in CH_2Cl_2 (50 ml), containing TFA (1 ml), phenylenetetramine **15** (100 mg) was added, and the reaction mixture stirred at room temperature for 5 days. The mixture was poured into water (500 ml), and the products were extracted with CH_2Cl_2 (3×50 ml). The extracts were combined and washed with 1% aqueous acetic acid (300 ml), then with water (2×300 ml), dried over sodium sulfate, and the solvent was removed under reduced pressure. The residue was chromatographed on a silica column eluting with 2% acetone/CH_2Cl_2 to give two fractions, which were purified by preparative TLC.

Dimer (16). Obtained from the reaction as a mobile orange–red band (15 mg; 23%), UV/vis (CH_2Cl_2): $\lambda_{max}(\epsilon)$=399 (82,000), 498 (10,900), 549 (41,000), 665 (26,000); 720 (70,500). NMR (600 MHz, $CDCl_3$): δ=−1.41 (br s, 4H, NH), 1.24 (t, 6H, CH_2CH_3), 1.90–2.64 (m, 8H, 17a/17a′, 17b/17b′-H), 1.92 (d, J=7.4 Hz, 6H, 18/18′CH_3), 3.62 (br s, 24H, OCH_3 and ring CH_3), 3.64 (q, 4H, CH_2CH_3), 4.67 (dq, J=7.4 Hz, 2H, 18/18′-H), 5.42 (dd, J=7.8 Hz, 2H, 17/17′-H), 6.28 (d, J=12 Hz, 2H, 3a/3a′-H), 6.37 (d, J=17 Hz, 2H, 3a/3a′-H), 7.88 (br s, 2H, benzene-H), 8.08 (dd, J=12, 17 Hz, 2H, 3b/3b′-H), 8.34 (s, 2H, 20/20′-H); 8.79 (s, 2H, 5/5′-H), 8.94 (br s, 2H, 10/10′-H). MS: m/z (%)=1192 (MH^+, 100%), 1045 (21%). HRMS (EI): calcd for $C_{74}H_{70}N_{12}O_4$: m/z 1191.5670; found: 1191.5653.

Dimer (17). Obtained from the reaction as a brown–red band (5 mg; 8%), UV/vis (CH_2Cl_2): $\lambda_{max}(\epsilon)$=378 (58,000); 459 (125,000); 567 (28,000); 678 (14,000); 744 (62,000). NMR (400 MHz, $CDCl_3$): δ=−1.22 (br s, 2H, NH); −0.74 (br s, 2H, NH); 1.29 (m, 6H, CH_2–CH_3) 1.90–2.60 (m, 8H, 17/17′a, b-H), 1.88 (m, 6H, 18/18′-CH_3), 3.61–3.69 (m, 28H, OCH_3, ring CH_3, CH_2–CH_3), 4.60 (q, 1H, 18′-H), 4.68 (q, 1H, 18-H); 5.39 (m, 1H, 17′-H), 5.59 (m, 1H, 17-H), 6.29 (m, 2H, 3a/3a′-H), 6.40 (m, 2H, 3a/3a′-H), 7.90 (m, 2H, 3b/3b′-H), 8.12 (br s, 2H, 20/20′-H), 8.20 (br s, 1H, benzene-H), 8.54 (br s, 1H, benzene-H), 8.68 (s, 1H, 5′-H), 8.70 (s, 1H, 5-H), 8.76 (br s, 1H, 10′-H), 8.81 (br s, 1H, 10-H). MS: m/z (%)=1207 (MH^+,

100%), 1179 (12%), 1118 (23%). HRMS (EI): calcd for $C_{74}H_{70}N_{12}O_5$: *m/z* 1207.5646; found: 1207.5702.

Crystal structure determinations

Crystals were grown by liquid diffusion and mounted on the diffractometer according to the method given by Hope.[31] For both data sets the intensities were corrected for Lorentz and polarization effects; an absorption correction was applied using the program XABS2.[32a] The two structures were solved by Direct Methods using the program SHELXS-97[32b] and refinements were carried out by full-matrixpleast-squares on [F^2] using the program SHELXL-97.[32c] Hydrogen atom were included at calculated positions using a riding model. The abolute structure for both compounds was assigned according to the one established for pheophorbide *a*, from which both compounds were formally derived.[33]

Crystal data for 5. $C_{40}H_{38}N_6O_3$, FW=650.76. Green plate, 0.5×0.4×0.1 mm^3, orthorhombic $P2_12_12$, a=14,929(9) Å, b=29.715(17) Å, c=7.295(1) Å, V=3236(3) Å^3, Z=4, p_{calc}=1.334, Siemens R3m/V diffractometer, O_{max}=25.01°, MoKα radiation, λ=0.71073 Å, ω-scans, T=126 K, 3301 measured reflections, 3274 independent reflections (R_{int}=0.0304), 1884 reflections with $I>2\sigma(I)$, 447 parameters, μ=0.085 mm^{-1}, R ($I>2\sigma(I)$=0.0603, R (all data)=0.1313, wR (all data)=0.1558, residual electron density=0.231e Å^{-3}. The carbonyl oxygen atom O_2 was refined as disordered over two split positions with equal occupancy.

Crystal data for 6. $C_{40}H_{38}N_6O_3$, FW=634.76. Blue Block, 0.8×0.8×0.4 mm^3, orthorhombic $P2_12_12$, a=13,791(5) Å, b=15.001(4) Å, c=15.554(6) Å, V=3216(3) Å^3, Z=4, p_{calc}=1.331, Siemens P4 diffractometer equipped with rotating anode O_{max}=56.64°, CuKα radiation, λ=1.54178, 3895 reflections with $I>2\sigma(I)$, 434 parameters, μ=0.655 mm^{-1}, R ($I>2\sigma(I)$=0.0577, R (all data)=0.0594, wR (all data)=0.1563, residual electron density=0.399e Å^{-3}. The carbonyl oxygen atom O_2 was refined as disordered over two split positions with equal occupancy.

Molecular modeling studies

SYBYL molecular modeling program version 6.3 (Tripos, St. Louis) running on Silicon Graphics Indigo 2 (R10000) was used to build the plausible structure for symmetrical dimer **16** on the basis of the crystallographically determined monomer structure **4**. The least square juxtaposition was performed by using the six-membered ring atoms in the middle of the linker region. Using standard SYBYL energy parameters, the structure was energy optimized using the distance dependent dielectric function and the σ Del Re and π Hückel charges. Similarly, a model for the unsymmetrical dimer was built from the crystallographic coordinates of the monomers **4** and **5**.

Acknowledgements

This work was supported by grants from the Mallinckrodt Medical Inc., St. Louis and the National Institutes of Health (CA 55791), the Oncologic Foundation of Buffalo and Council of Scientific Industrial Research (CSIR), New Delhi, India, and from the Deutsche Forschungsgemeinschaft (Se543/2-4 and Heisenberg scholarship to M.O.S.), the Fonds der Chemischen Industrie (M.O.S.). We thank Dr J. L. Alderfer, Molecular and Cellular Biophysics, RPCI, Buffalo, for 2D ROESY NMR studies. Partial support to the NMR Facility by RPCI Center Support Grant (CA 16056) is also acknowledged.

References

1. A part of this work was published as a communication: Kozyrev, A. N.; Alderfer J. L.; Srikrishnan, T.; Pandey, R. K.; *J. Chem. Soc. Perkin Trans. 1* (communication) **1998**, 837–838.
2. (a) Pandey, R. K.; Zheng, G. Porphyrins as Photosensitizers in Photodynamic Therapy. In *The Porphyrin Handbook*; Kadish, Smith and Guilard, Eds.; Academic Press: New York, 2000; Vol. 6. (b) Pandey, R. K.; Herman, C. *Chem. & Industry (London)* **1998**, 739–743.
3. Krattinger, B.; Nurco, D. J.; Smith, K. M. *Chem. Commun.* **1998**, 757–758.
4. Johnson, C. K.; Dolphin, D. *Tetrahedron Lett.* **1998**, *39*, 4619–4622.
5. Mettah, S.; Shibata, M.; Alderfer, J. L.; Senge, M. O.; Smith, K. M.; Rein, R.; Dougherty, T. J.; Pandey, R. K. *J. Org. Chem.* **1998**, *63*, 1646–1656.
6. Faustino, M. A.; Neves, M. G. P. S.; Vicente, M. G. H.; Silva, A. M. S.; Cavaleiro, J. A. S. *Tetrahedron Lett.* **1995**, *36*, 5977–5980.
7. Garbo, G. *J. Photochem. Photobiol. B: Biology* **1996**, *34*, 109–116.
8. Kozyrev, A. N.; Zheng, G.; Zhu, C.; Dougherty, T. J.; Smith, K. M.; Pandey, R. K. *Tetrahedron Lett.* **1996**, *37*, 6431–6434.
9. Pandey, R. K.; Jagerocic, N.; Ryan, J. M.; Dougherty, T. J.; Smith, K. M. *Tetrahedron* **1996**, *52*, 5349–5362.
10. Potter, W. R.; Henderson, B. W.; Bellnier, D. A.; Pandey, R. K.; Vaughan, L. A.; Weishaupt, K. R.; Dougherty, T. J. *J. Photochem. Photobiol.* **1999**, *70*, 781–788.
11. Senge, M. *J. Photochem. Photobiol.* **1992**, 3–36.
12. Kozyrev, A. N.; Alderfer, J. L.; Dougherty, T. J.; Pandey, R. K. *Chem. Commun.* **1998**, 1083–1084.
13. Kozyrev, A. N.; Dougherty, T. J.; Pandey, R. K. *Chem. Commun.* **1998**, 481–482.
14. Reek, J. N. H.; Rowan, A. E.; Gelder, R.; Beurskens, P. T.; Crossley, M. J.; Feyer, S. D.; Schryver, F.; Nolte, R. J. M. *Angew. Chem Int. Ed., Engl.* **1997**, *36*, 36 (and references therein).
15. Sessler, J. L.; Hemmi, G.; Mody, T. D.; Murai, T.; Burrell, A.; Young, S. W. *Acc. Chem. Res.* **1994**, 43–50 (and references therein).
16. Jaquinod, J.; Senge, M. O.; Pandey, R. K.; Forsyth, T. P.; Smith, K. M. *Angew. Chem. Int. Ed. Engl.* **1996**, *35*, 1840.
17. Hynninen, P. *Chemistry of Chlorophylls: Modifications in 'Chlorophylls'*; Scheer, H., Ed.; CRC Press: Boca Raton, FL, 1990.
18. Wasielewski, M. R. *Chem. Rev.* **1992**, *92*, 435–461 (and references therein).
19. (a) Lehn, J. M. *Supramolecular Chemistry*; VCH: Weinhein, 1995. (b) Norris, J. R., Deisenhofer, J., Eds.; *The Photosynthetic Reaction Center*; Academic Press: San Diego, 1993. (c) Jaquinod, L.; Nurco, D. J.; Pandey, R. K.; Senge, M. O.; Smith, K. M. *Angew. Chem. Int. Ed. Engl.* **1996**, *35*, 2496–2499.
20. (a) Crossley, M. J.; Langford, S. J.; Parashar, J. K.; Burn, P. L.

J. Chem. Soc., Chem. Commun. **1995**, 1921–1923. (b) Wagner, R. W.; Lindsey, J. S. *J. Am. Chem. Soc.* **1994**, *116*, 9759–9760. (c) Sessler, J. L.; Johnson, M. R.; Lin, T. Y.; Greager, S. E. *J. Am. Chem. Soc.* **1988**, *110*, 3659–3661. (d) Chang, C. K.; Abdalmuhdi, I. *J. Org. Chem.* **1983**, *48*, 5388–5390. (e) Gust, D.; Moore, T. A. *Science* **1989**, *244*, 35–41. (f) Pandey, R. K.; Forsyth, T. P.; Gerzevske, K. R.; Lin, J. L.; Smith, K. M. *Tetrahedron Lett.* **1992**, *33*, 5515–5318. (g) Jaquinod, L.; Nurco, D. J.; Medforth, C. J.; Pandey, R. K.; Forsyth, T. P.; Olmstead, M.; Smith, K. M. *Angew. Chem. Int. Ed. Engl.* **1996**, *35*, 1013–1016.

21. Ma, L.; Dolphin, D. *J. Org. Chem.* **1996**, *61*, 2501–2510.

22. Lee, S. H.; Jagerovich, N.; Smith, K. M. *J. Chem. Soc., Perkin Trans. 1* **1993**, 2369–2377.

23. Kumar, C. V.; Qin, L.; Das, P. K. *J. Chem. Soc. Faraday Trans.* **1984**, *80* (2), 783–793.

24. Carmichael, I.; Hug, G. L. *J. Phys. Chem. Ref. Data* **1986**, *15*, 1–250.

25. Gandin, E.; Lion, Y.; de Vorst, V. *Photochem. Photobiol.* **1983**, *37*, 271–278.

26. *Handbook of Organic Photochemistry*, Scaiano, J. C., Ed.; CRC Press: Boca Raton, FL, 1989, pp 229–247.

27. Foote, C. S. *Singlet Oxygen*, Academic Press: New York, 1979.

28. Merker, P. B.; Kearns, D. R. *J. Am. Chem. Soc.* **1975**, *97*, 462–463.

29. Eastman Kodak Company, *Kodak Laser Dyes*, Kodak: New York, 1987.

30. Ramaiah, D.; Joy, A.; Chandrasekhar, N.; Eldho, N. V.; Das, S.; George, M. V. *Photochem. Photobiol.* **1997**, *65*, 783–790.

31. Hope, H. *Prog. Inorg. Chem.* **1994**, *41*, 1.

32. (a) Parkin, S. R.; Moezzi, B.; Hope, H. *J. Appl. Crystallogr.* **1995**, *28*, 53. (b) Sheldrick, G. M. *SHELXS-97*: Program for Crystal Structure Solution; Universitat Gottingen, 1997. (c) Sheldrick, G. M. *SHELXL-97*: Program for Crystal Structure Refinement; Universitat Gottingen, 1997.

33. The authors have deposited atomic coordinates and a full structure description with the Cambridge Crystallographic Data Centre. The structures can be obtained, upon request, from the Director, Cambridge Crystallographic Data Centre, 12 Union Road, Cambridge CB2 1EZ, UK.